TRPV1 promotes opioid analgesia during inflammation

Lilian Basso, Reem Aboushousha, Churmy Yong Fan, Mircea Iftinca, Helvira Melo, Robyn Flynn, Francina Agosti, Morley D Hollenberg, Roger Thompson, Emmanuel Bourinet, et al.

PAIN

TRPV1 promotes opioid analgesia during inflammation

Lilian Basso[1], Reem Aboushousha[1], Churmy Yong Fan[2], Mircea Iftinca[1], Helvira Melo[1], Robyn Flynn[1], Francina Agosti[3], Morley D. Hollenberg[1], Roger Thompson[2], Emmanuel Bourinet[3], Tuan Trang[2], Christophe Altier[1]*

Pain and inflammation are inherently linked responses to injury, infection, or chronic diseases. Given that acute inflammation in humans or mice enhances the analgesic properties of opioids, there is much interest in determining the inflammatory transducers that prime opioid receptor signaling in primary afferent nociceptors. Here, we found that activation of the transient receptor potential vanilloid type 1 (TRPV1) channel stimulated a mitogen-activated protein kinase (MAPK) signaling pathway that was accompanied by the shuttling of the scaffold protein β-arrestin2 to the nucleus. The nuclear translocation of β-arrestin2 in turn prevented its recruitment to the μ-opioid receptor (MOR), the subsequent internalization of agonist-bound MOR, and the suppression of MOR activity that occurs upon receptor desensitization. Using the complete Freund's adjuvant (CFA) inflammatory pain model to examine the role of TRPV1 in regulating endogenous opioid analgesia in mice, we found that naloxone methiodide (Nal-M), a peripherally restricted, nonselective, and competitive opioid receptor antagonist, slowed the recovery from CFA-induced hypersensitivity in wild-type, but not TRPV1-deficient, mice. Furthermore, we showed that inflammation prolonged morphine-induced antinociception in a mouse model of opioid receptor desensitization, a process that depended on TRPV1. Together, our data reveal a TRPV1-mediated signaling pathway that serves as an endogenous pain-resolution mechanism by promoting the nuclear translocation of β-arrestin2 to minimize MOR desensitization. This previously uncharacterized mechanism may underlie the peripheral opioid control of inflammatory pain. Dysregulation of the TRPV1–β-arrestin2 axis may thus contribute to the transition from acute to chronic pain.

INTRODUCTION

Pain modulation and inflammation are two integrated biological responses that function in cooperation after injury. Particularly known for their analgesic properties, opioids target receptors expressed throughout the afferent pain pathway, including central and peripheral nerve terminals of primary afferent neurons (*1*–*3*). Drugs and local endogenously produced opioids, β-endorphin, enkephalins, and dynorphins, exert efficient inhibitory control of pain at both spinal (*1*, *2*) and peripheral sites after inflammation (*4*–*8*). At inflammatory sites, immune-derived opioids are released to counteract pain effectively and facilitate healing. Moreover, an alteration in the endogenous opioid system in the spinal cord was proposed to prevent the transition from acute inflammatory to chronic pain (*1*), particularly through tonic μ-opioid receptor (MOR) activity that suppresses hyperalgesia after resolution of inflammation. Thus, both endogenous and xenobiotic opioids are most effective immediately after tissue injury, suggesting that the early phases of inflammation primes opioid receptor signaling in nociceptive afferent neurons (*7*, *9*). Alterations in this priming might contribute to a decrease in the therapeutic window of opioids, requiring increased analgesic doses that can lead to side effects. Accordingly, at sites of acute local inflammation in humans or mice, the analgesic properties of opioids are enhanced (*10*), whereas application of opioids to a human peripheral nerve plexus does not elicit analgesia in non-inflamed tissue (*11*). At these sites, the transient receptor potential vanilloid type 1 (TRPV1) channel is the main endpoint target of inflammatory mediators, including reactive oxygen species, metabolites of polyunsaturated fatty acids, and protons or toxins released by pathogens that directly activate (*12*) and sensitize the channel by G protein–coupled receptor (GPCR)–targeted mediators (bradykinin, prostaglandin E_2, and proteases) (*13*–*16*). These inflammatory processes, in turn, cause hyperalgesia during tissue inflammation (*17*) and in many immune-associated diseases (*12*, *18*–*21*).

Along these lines, previous work reported functional interactions between the signaling pathways of TRPV1 and MORs, and findings suggest that MORs found in $TRPV1^+$ primary afferent nociceptors are essential contributors to analgesic tolerance (*22*); however, the underlying molecular mechanisms remain unknown. We set out to test whether TRPV1 could prime opioid-induced antinociception by minimizing receptor desensitization and enhancing opioid receptor signaling. As a central regulator of MOR function and desensitization, the role of β-arrestin2 was investigated in relation to TRPV1 activation. We found that, upon treating TRPV1-expressing human embryonic kidney (HEK) cells with capsaicin, the active component of chili peppers that binds to the channel, β-arrestin2 is trafficked to the nucleus through a calcium-dependent mitogen-activated protein kinase (MAPK) signaling pathway. As a result of this exclusion of β-arrestin2 from the cytosol, activated MORs were unable to recruit β-arrestin2 and become internalized during agonist-induced desensitization. Using the complete Freund's adjuvant (CFA) inflammatory pain model, we then investigated the role of TRPV1 in both endogenous and exogenous opioid-induced antinociception.

Although TRPV1, MOR, and β-arrestin2 are well-known players in inflammatory pain and analgesia, our data uncover an unappreciated mechanism whereby inflammation-mediated activation of TRPV1 might minimize the desensitization of opioid receptors to enhance analgesia. This TRPV1 opioid receptor interaction could be pharmacologically targeted in clinical settings to improve pain management by opioids.

[1]Department of Physiology and Pharmacology, Inflammation Research Network-Snyder Institute for Chronic Diseases and Alberta Children's Hospital Research Institute, Cumming School of Medicine, University of Calgary, Calgary, Alberta T2N4N1, Canada. [2]Hotchkiss Brain Institute, Cumming School of Medicine, Faculty of Veterinary Medicine, University of Calgary, Calgary, Alberta T2N4N1, Canada. [3]Institute for Functional Genomics, CNRS UMR5203, INSERM U1191, University of Montpellier, LABEX ICST, Montpellier, France.
*Corresponding author. Email: altier@ucalgary.ca

RESULTS

TRPV1 activation induces both β-arrestin2 nuclear localization and extracellular signal–regulated kinase 1 and 2 phosphorylation

Previous work showed that β-arrestin2 functionally interacts with TRPV1 (*23*), and other findings revealed that TRPV1 activation blocks opioid-dependent phosphorylation of MOR (*24*). We thus asked whether channel activation could, through competitive interaction, prevent the recruitment of β-arrestin2 to the opioid receptor at the plasma membrane. Using spinning disk confocal microscopy on TRPV1-expressing HEK cells, we first examined the fate of the yellow fluorescent protein (YFP)–fused β-arrestin2 (β-arrestin2–YFP) after channel activation. Although we expected β-arrestin2 to accumulate at the plasma membrane, stimulation of TRPV1 by resiniferatoxin (RTX) or capsaicin promoted a rapid translocation of β-arrestin2 to the nucleus (Fig. 1, A and B). Image quantification indicated that >70 and ~50% of TRPV1-mCherry–expressing cells displayed nuclear translocation of β-arrestin2 after 15 min of TRPV1 stimulation by RTX or capsaicin, respectively (Fig. 1C and fig. S1A). This translocation was slowly reversed upon washout of capsaicin, did not occur in the absence of the channel (fig. S1, A and B), and specifically targeted the nucleus, as confirmed by staining of nuclei with Hoechst blue in TRPV1-stimulated cells (fig. S1C). To get a more precise analysis of the time course of the effect, we assessed β-arrestin2 translocation by bystander bioluminescence resonance energy transfer (BRET) assay (*25*) using β-arrestin2 conjugated to *Renilla* luciferase (rLuc) coexpressed with the *Renilla* green fluorescent protein (rGFP) fused to the nuclear localization sequence (NLS) PKKKRKVEDPKS, which targets the nucleus (Fig. 1D). As was previously reported, this BRET approach enables the trafficking of proteins in the same subcellular compartments to be monitored and thus quantitatively assesses the nuclear translocation of β-arrestin2 after channel stimulation in a concentration- and time-dependent manner. When TRPV1 was expressed, increasing the concentration of capsaicin at 37°C induced an increase in bystander BRET signal between βARR2-rLuc and rGFP-NLS, which indicated the accumulation of β-arrestin2 in the nucleus, in proximity to the rGFP-NLS (Fig. 1, E and F). This effect depended on the presence of TRPV1 (fig. S1D), occurred at concentrations of capsaicin >10 nM, with 2 min of channel activation, and reached a plateau at ~12 min after treatment (Fig. 1E). In contrast, TRPA1, another calcium-permeant member of the TRP channel family, failed to mediate β-arrestin2 accumulation in the nucleus (fig. S1, E and F), thus highlighting a specific TRPV1-driven calcium signaling pathway that caused β-arrestin2 translocation.

Arrestins are important scaffolds for the MAPK/extracellular signal–regulated kinase 1 (ERK1) and ERK2 (hereafter, ERK1/2) signaling pathway, which is also sensitive to the intracellular Ca^{2+} concentration. We thus tested the effect of TRPV1 stimulation on the activation of ERK1/2. In TRPV1-expressing HEK 293 cells, RTX induced a transient phosphorylation (and thus activation) of ERK1/2 at 5 min after stimulation (Fig. 1, G and H). ERK1/2 activation was blocked by chelating extracellular Ca^{2+} with 10 mM EGTA (Fig. 1I), which also prevented β-arrestin2 nuclear translocation (Fig. 1J), suggesting that Ca^{2+} influx through activated TRPV1 mediates both processes. Although different isoforms of protein kinase C (PKC) are implicated upstream of ERK1/2 activation (*26*, *27*), we found that pharmacological inhibition of PKC–beta II (PKCβII) by CGP53353 blocked ERK1/2 phosphorylation in response to TRPV1 stimulation, whereas selective inhibition of the α or βI isoforms with GF109203X did not (fig. S1, G and H). Accordingly, TRPV1 activation by RTX seemed to directly activate PKCβII (fig. S1I). Together, these findings suggest that the activation of TRPV1 engages a signaling cascade involving both the Ca^{2+}- and PKCβII-dependent activation of ERK1/2, which coincides with the translocation of β-arrestin2 to the nucleus.

TRPV1 activation disrupts the MOR–β-arrestin2 interaction and receptor internalization

To determine whether TRPV1-induced translocation of β-arrestin2 would prevent its recruitment to the activated MOR, we monitored the interaction of the *Renilla* luciferase–fused MOR (MOR-Rluc8) with the Venus fluorescent protein–fused β-arrestin2 (β-arrestin2–Venus) using BRET1 assay in HEK 293 cells. Activation of MOR with its specific synthetic opioid peptide DAMGO ([D-Ala2, N-MePhe4, Gly-ol]-enkephalin) induced the recruitment of β-arrestin2 to MOR (Fig. 2), as indicated by an increase in BRET signal that plateaus after 400 s of treatment. In the absence of TRPV1, application of 500 nM capsaicin did not induce a BRET response or affect the DAMGO-induced recruitment of β-arrestin2 to MOR. However, in TRPV1-expressing cells, whereas capsaicin alone had no effect, cotreatment with 10 μM DAMGO completely blocked the interaction between MOR and β-arrestin2 (Fig. 2, B and C). This effect was observed at low and even saturating concentrations of DAMGO (Fig. 2D). Furthermore, use of the reversed pair of BRET biosensors (βARR2-Rluc + MOR-YFP) yielded similar results (fig. S2), thus confirming the inhibitory effect of TRPV1 activation on MOR–β-arrestin2 interaction. Moreover, coimmunoprecipitation of MOR with TRPV1 indicated the formation of a receptor-channel signaling complex at steady state, which was unaffected by DAMGO treatment (Fig. 2E), and saturating BRET signals obtained for coexpression of channel and receptor suggested a close interaction between MOR and TRPV1, with or without DAMGO (Fig. 2F). Therefore, our data show that proximity of TRPV1 to MOR alters the β-arrestin2–biased agonism of DAMGO by redirecting β-arrestin2 or preventing its recruitment to the receptor upon channel activation. We also found that this mechanism applies to other neuronal GPCRs, because the proteinase-activated receptor-2 (PAR2), which like MOR is involved in inflammatory pain, showed impaired β-arrestin2 recruitment after cotreatment with capsaicin (fig. S2, D and E).

Given that β-arrestin2 is an essential modulator of MOR desensitization and recycling, we next tested the functional outcome of TRPV1 activation on receptor internalization. Using confocal microscopy, we found that, as previously reported, exposure to 1 μM DAMGO for 20 min promoted robust receptor internalization in HEK 293 cells expressing MOR-YFP and TRPV1-mCherry. In contrast, cells costimulated with DAMGO and capsaicin (or DAMGO + RTX; fig. S3A) had less internalized receptors (Fig. 3, A and B). Imaging of cells expressing β-arrestin2–YFP, TRPV1–cyan fluorescent protein (CFP), and MOR-mCherry revealed that, upon DAMGO treatment, β-arrestin2 colocalized with internalized MOR-containing vesicles (fig. S3A, middle panels). After combined application of DAMGO with RTX however, β-arrestin2 sequestered in the nucleus, because of channel stimulation, thus preventing the agonist-induced internalization of MOR (Fig. 3, A and B, and fig. S3A, bottom panels). Deletion of β-arrestin2 using a CRISPR β-arrestin2 knockout cell line (fig. S3B) eliminated DAMGO-evoked internalization and thus mimicked the DAMGO with capsaicin condition in β-arrestin2 wild-type (WT) cells (fig. S3C). Next, using a quantitative bystander BRET assay developed by Namkung *et al.*

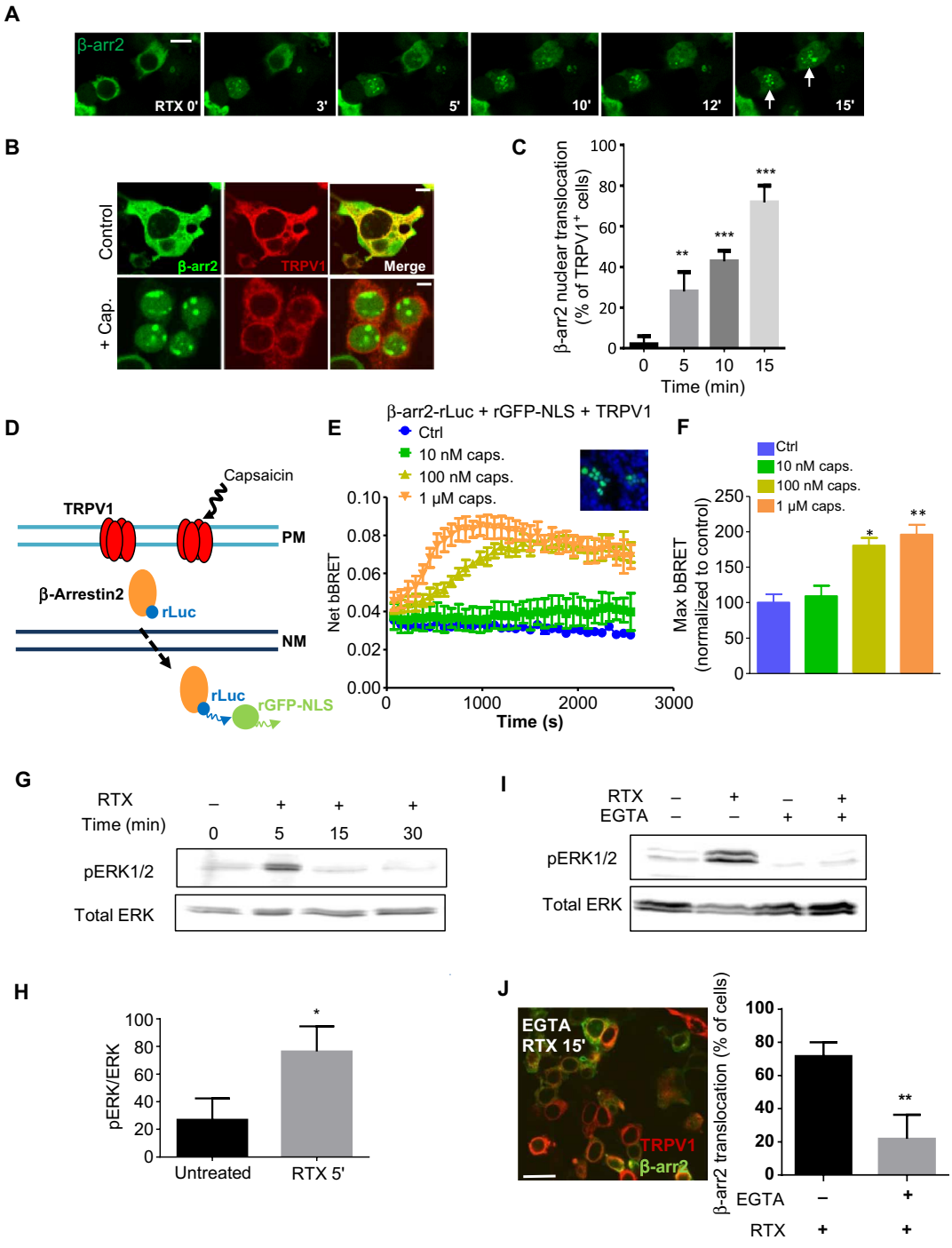

Fig. 1. Activation of TRPV1 mediates translocation of β-arrestin2 to the nucleus. (**A** to **C**) Spinning disk confocal imaging (A and B) and quantification (C) of β-arrestin2 nuclear translocation in HEK cells transfected with plasmids expressing TRPV1-mCherry (red; B) and β-arrestin2–YFP (green) and treated with either bath-applied 10 nM RTX at 37°C for the indicated times (A) or 1 μM capsaicin for 15 min (B). Arrows (A) indicate the nuclear localization of β-arrestin2–YFP. Scale bars, 10 μm. Data (C) are means ± SEM of at least 100 cells per condition from five experiments. $^{**}P < 0.001$ and $^{***}P < 0.0001$ compared to time zero by an unpaired *t* test. (**D**) Illustration of the bystander BRET assay used to monitor the trafficking of β-arrestin2 to the nucleus. PM, plasma membrane; NM, nuclear membrane. (**E** and **F**) Time course of net bystander (E) and maximum (F) BRET measured in HEK cells expressing TRPV1, β2ARR-rLucII, and *Renilla* GFP-NLS and exposed to various concentrations of capsaicin (caps.) injected at time zero. Inset: Image of nuclear localization of the GFP-NLS signal in cells costained with 4′,6-diamidino-2-phenylindole (DAPI). In (F), data were normalized to control (ctrl; vehicle) conditions and are means ± SEM of three experiments. $^{*}P < 0.05$ and $^{**}P < 0.001$ by one-way analysis of variance (ANOVA) and Bonferroni post hoc test. (**G** and **H**) Western blotting and analysis of phosphorylated and total ERK in HEK cells transfected with plasmid expressing TRPV1 and treated with 10 nM RTX for the indicated times. Blots are representative of three experiments; data are means ± SEM of three experiments. (**I** and **J**) Effect of the Ca^{2+}-chelator EGTA (10 mM) on RTX-induced pERK1/2 at 5 min as assessed by Western blotting (I) and on RTX-induced β-arrestin2 nuclear translocation at 15 min as assessed by confocal microscopy (J). Scale bar, 20 μm. Blots and image are representative of three experiments; data are means ± SEM of three experiments. $^{*}P < 0.05$; $^{**}P < 0.01$ by unpaired *t* test.

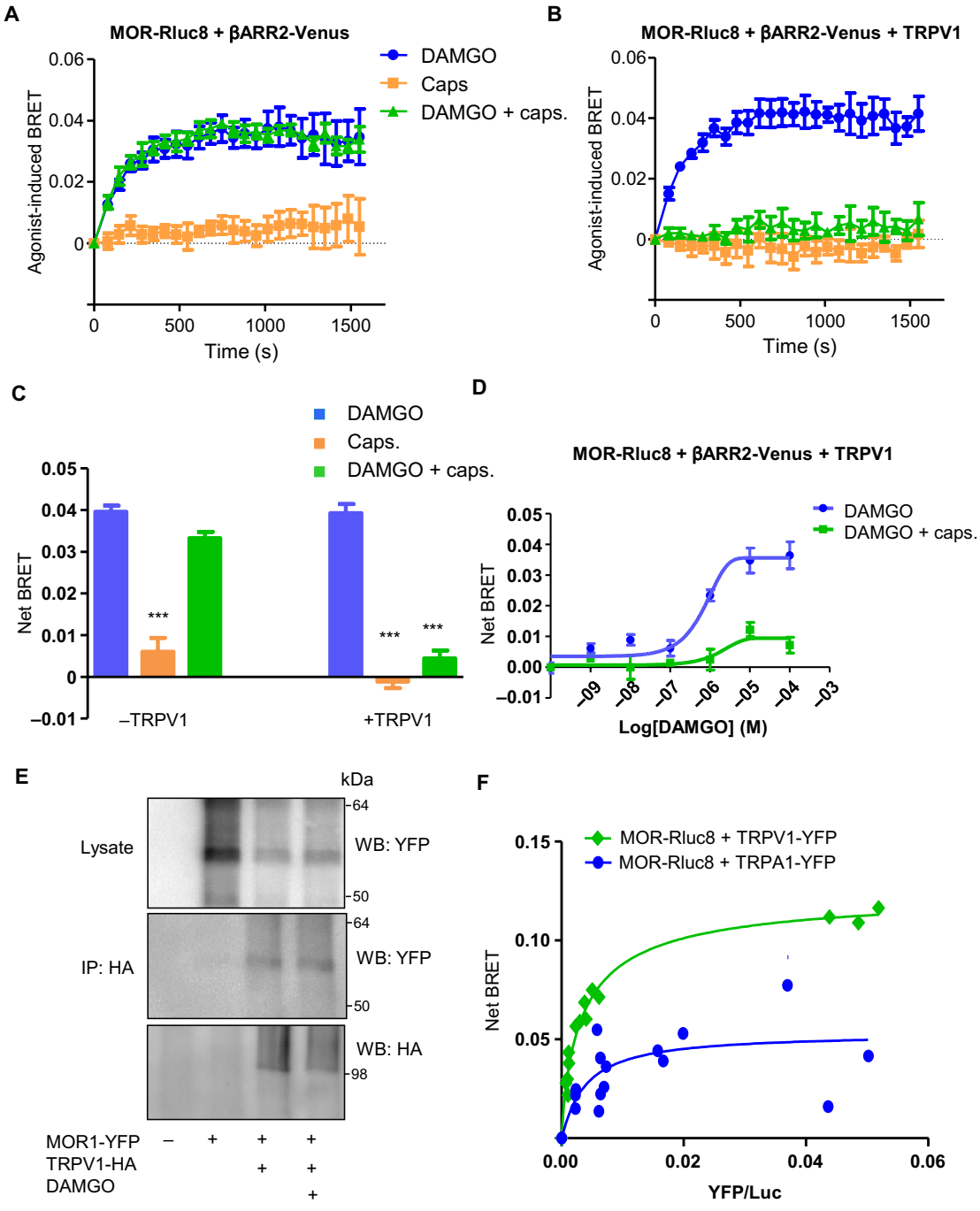

Fig. 2. Activation of TRPV1 prevents the DAMGO-induced interaction between MOR and β-arrestin2. (**A** and **B**) BRET measured over time in HEK cells expressing MOR-Rluc8 and β-arrestin2–Venus (βARR2-Venus) and exposed to 10 μM DAMGO (blue), 500 nM capsaicin (red), or both (green) injected a time zero, either in the absence (A) or presence (B) of TRPV1 expression. Data are means ± SEM of three experiments. (**C**) Quantification of the BRET signal, obtained from the experiments represented in (A) and (B). Data are means ± SEM of the last four points on the time-course curve, from three experiments. ***$P < 0.001$. (**D**) Dose-response curve of the net BRET between MOR-Rluc8 and β-arrestin2–Venus in the cells described in (B) exposed to increasing concentration of DAMGO (blue) or DAMGO and capsaicin (green). (**E**) Co-immunoprecipitation (IP) from HEK cells expressing MOR-YFP alone or with TRPV1-hemagglutinin (HA) and exposed to vehicle (lanes 1 to 3) or 1 μM DAMGO (lane 4). Blot is representative of three experiments. WB, Western blot. (**F**) Net BRET saturation curves between MOR-Rluc8 and TRPV1-YFP or TRPA1-YFP in HEK cells. Data are representative of three independent experiments.

(*25*), we took advantage of the rGFP-tagged FYVE domain of endofin (Q739-K806) to monitor receptor internalization into early endosomes (Fig. 3C) upon treating HEK 293 cells with DAMGO or DAMGO and capsaicin. Activation of MOR by 1 μM DAMGO at 37°C induced an increase in bystander BRET signal between MOR-Luc8 and rGFP-FYVE selectively targeted to intracellular vesicles. The degree of receptor internalization peaked at ~15 min after DAMGO application and then plateaus. In contrast, as observed

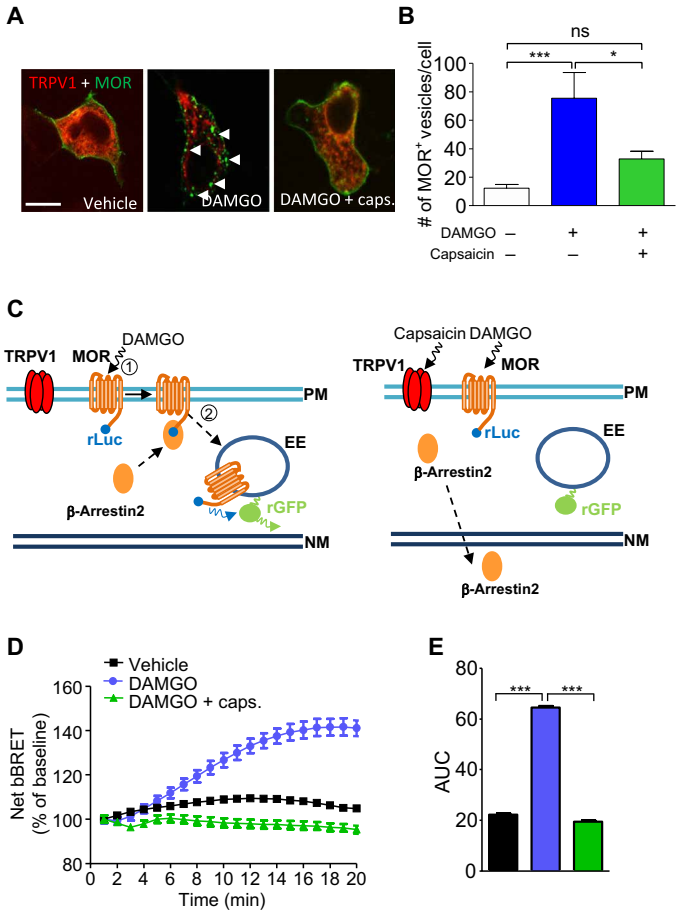

Fig. 3. Activation of TRPV1 prevents MOR internalization. (**A** and **B**) Confocal microscopy of HEK cells expressing MOR-YFP (green) and TRPV1-mCherry (red) exposed to vehicle, 10 μM DAMGO, or 10 μM DAMGO and 1 μM capsaicin for 30 min. Scale bar, 10 μm. Number of MOR^+ vesicles per cell (white arrows) were counted with ImageJ software. Data are means ± SEM of at least 100 cells per condition from three independent experiments. $^*P < 0.05$ and $^{***}P < 0.001$ by Kruskal-Wallis test followed by Dunn's post hoc test. ns, not significant. (**C**) Illustration of the bystander BRET-based approach for monitoring MOR trafficking to FYVE-tethered early endosomes (EE) in response to DAMGO or DAMGO and capsaicin. Upon treatment with DAMGO, the internalized MOR-rLuc8 induces an increase in BRET signal compared to unstimulated condition (left). On the basis our observations in (A), cotreatment with DAMGO and capsaicin (right) will reduce the BRET response by preventing receptor trafficking to FYVE-tethered early endosomes. (**D**) Bystander net BRET over time in HEK cells exposed to vehicle [phosphate-buffered saline (PBS)] or 10 μM DAMGO at 37°C for 20 min. Data were normalized to their respective baseline and are the means ± SEM from three experiments. (**E**) Bar graph representing the area under the curve (AUC) of the net bBRET data presented in (D). $^{***}P < 0.01$ by unpaired *t* test.

with confocal imaging, capsaicin cotreatment was able to blunt the internalization of MOR in early endosomes (Fig. 3, D and E).

TRPV1 activation prevents MOR desensitization

To assess the functional consequence of β-arrestin2 nuclear translocation on MOR function and desensitization, we measured the inhibition of N-type voltage-gated calcium channel (VGCC), as a surrogate of MOR-induced $G_{i/o}$ protein activation. In WT HEK 293 cells expressing TRPV1 with MOR and the $Ca_v2.2$ subunit, activation of MOR by 1 μM DAMGO induced a rapid and robust inhibition of $Ca_v2.2$ current (Fig. 4). This inhibition was not observed in the absence of MOR or in response to TRPV1 activation by capsaicin (fig. S4A), confirming that $Ca_v2.2$ responded specifically to DAMGO-bound MOR but not to TRPV1 activation. Desensitization of MOR by DAMGO preincubation for an hour prevented the acute DAMGO-induced modulation of $Ca_v2.2$ currents (Fig. 4, A and B). This effect was relieved by prolonged washout of DAMGO to allow recycling of internalized MOR (fig. S4B). Furthermore, preincubation with a combination of DAMGO and capsaicin could restore the acute MOR-promoted $Ca_v2.2$ inhibition (Fig. 4, A and B), an effect lost in the absence of TRPV1 (fig. S4C). In contrast, MOR activation resulted in a robust $Ca_v2.2$ inhibition in β-arrestin2 knockout (*ARRB2*$^{-/-}$) HEK 293 cells, despite pretreatment with DAMGO or DAMGO and capsaicin, supporting our hypothesis that β-arrestin2 translocation is essential in driving the TRPV1-induced blockade of MOR desensitization. Reintroducing β-arrestin2 to *ARRB2*$^{-/-}$ HEK cells reestablished receptor desensitization and its relief triggered by TRPV1 activation (Fig. 4, A and B).

TRPV1-induced translocation of β-arrestin2 occurs in dorsal root ganglion nociceptors

To examine β-arrestin2 translocation in TRPV1-expressing neurons, we immunostained acutely dissociated dorsal root ganglion (DRG) neurons from YFP-fused channel rhodopsin-2 that was expressed in TRPV1-lineage neurons (TRPV1-ChR2-EYFP). Whereas the subcellular distribution of β-arrestin2 was cytosolic in naïve DRG neurons of all sizes, capsaicin rapidly translocated β-arrestin2 into the nucleus, an effect that was only observed in YFP^+ neurons (Fig. 5, A and B). When looking at the functional effect of MOR activity in DRG neurons, we found that both WT and *TRPV1*$^{-/-}$ neurons exhibited inhibition of N-type calcium current in response to acute 1 μM DAMGO (Fig. 5, C and D). However, desensitization of the receptor by prolonged exposure (1 hour) to DAMGO canceled out the acute inhibitory effect of DAMGO on N-type channels in both WT and *TRPV1*$^{-/-}$ neurons (Fig. 5D). As found in heterologous expression systems, preincubation with a combination of DAMGO and capsaicin (100 nM) restored N-type inhibition induced by acute MOR activation (Fig. 5D). This effect occurred in $TRPV1^+$, capsaicin-responsive DRG neurons from WT animals. However, capsaicin cotreatment could not restore MOR-induced N-type inhibition in *TRPV1*$^{-/-}$ neurons (Fig. 5D). Overall, these data suggest that activation of TRPV1 minimizes desensitization of MOR in a β-arrestin2–dependent fashion.

TRPV1 stimulates endogenous opioid-mediated analgesia during inflammation

Given that TRPV1 is a central integrator of inflammatory signals (*28*–*30*), we tested whether the TRPV1-MOR interaction that we described in vitro regulated opioid analgesia in vivo. TRPV1 is likely the best-characterized sensory transducer expressed in polymodal C fibers, which process both thermal and mechanical hyperalgesia during long-lasting inflammation (*31*). Using the CFA model of chronic inflammatory pain, we evaluated peripheral immune-derived endogenous opioid antinociception (*6*, *32*–*35*) in WT and *TRPV1*$^{-/-}$ mice by measuring paw withdrawal threshold (PWT) during the acute and later (resolution) phase of inflammation. In WT animals, PWT was decreased by 50% at day 4 after intraplantar injection of CFA, and animals started to recover at day 6. Treatment with naloxone methiodide (Nal-M), a peripherally restricted nonselective

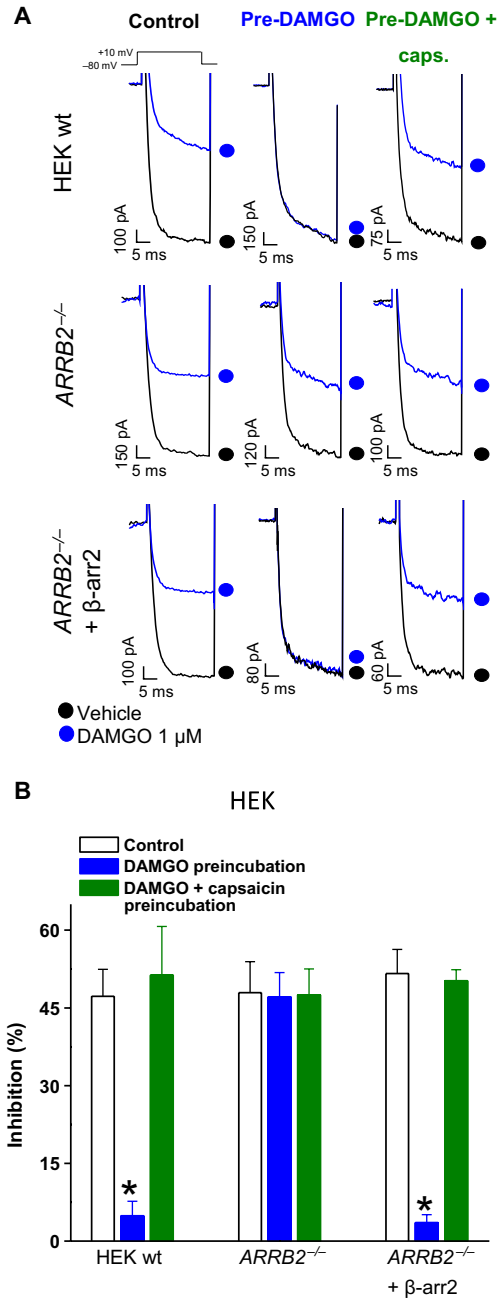

Fig. 4. Activation of TRPV1 prevents acute desensitization of DAMGO-mediated inhibition of the $Ca_v2.2$ current. (**A**) Representative $Ca2^+$ current traces (evoked at +10 mV from a holding potential of −80 mV during 30 ms) in HEK cells expressing $Ca_v2.2$ (+α2δ1 and β2a), MOR1, and TRPV1 and acutely treated with vehicle (black symbol) or 1 μM DAMGO (blue symbol). The current was recorded in control conditions (left traces), after 1 hour of preincubation with 1 μM DAMGO (middle traces, acute desensitization), and 1 hour after preincubation with 1 μM DAMGO and 100 nM capsaicin (right traces). Experiments were repeated using β-arrestin2 knockout (*ARRB2*$^{-/-}$) HEK cells with or without transfection with β-arrestin2 expression plasmid. Traces are representative of three independent experiments. (**B**) Percentage of peak current inhibition induced by 1 μM DAMGO in untreated (white), DAMGO-pretreated (blue), or DAMGO and capsaicin–pretreated cells (green) at 37°C. Data are means ± SEM from three independent experiments, from (left to right) 15, 9, 9, 10, 9, 10, 9, 10, and 10 HEK cells. *$P < 0.01$ by one-way ANOVA and Bonferroni post hoc test.

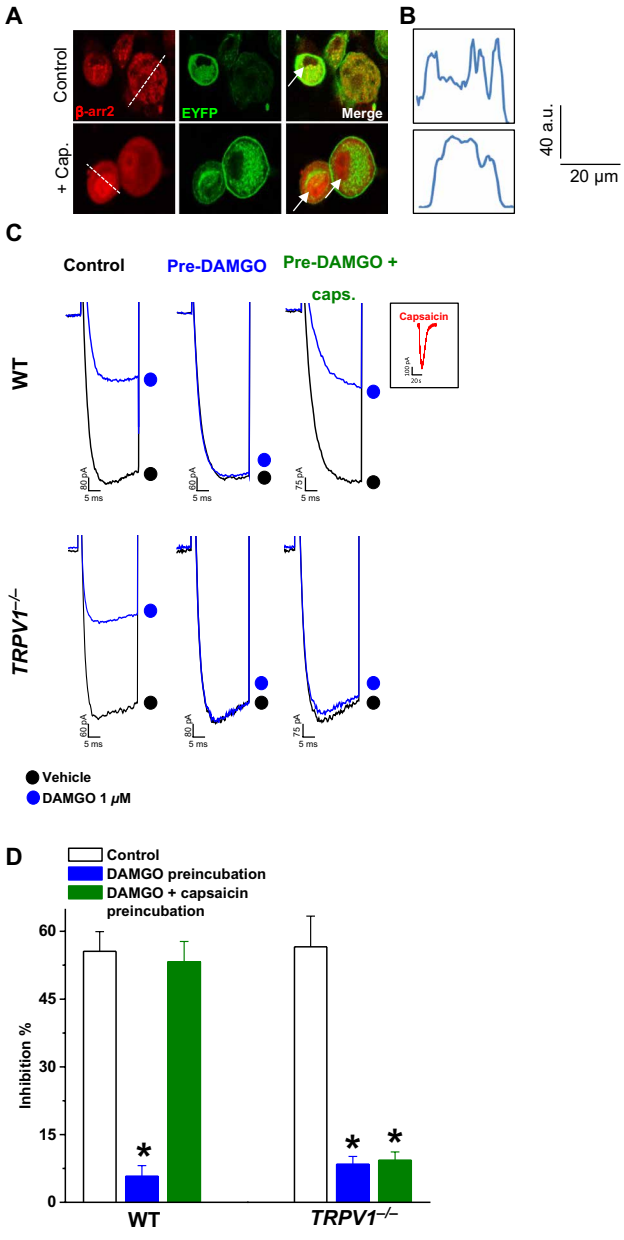

Fig. 5. Activation of TRPV1 promotes β-arrestin2 nuclear translocation, which results in reduced MOR desensitization in DRG neurons. (**A**) Representative confocal microscopy images of β-arrestin2 immunostaining (red) in TRPV1-expressing DRG neurons (green) isolated from Ai32/TRPV1-cre mice. Neurons were untreated (control) or stimulated with 100 nM capsaicin for 10 min. Images are representative of five independent experiments. (**B**) Linescan corresponding to the image in (A) and representing β-arrestin2 cellular distribution. a.u., arbitrary units. (**C**) Representative N-type current traces (recorded in the presence of 10 μM nifedipine) from a capsaicin-sensitive DRG neuron upon application of vehicle (black symbol) or 1 μM DAMGO (blue symbol). Recordings were done in DRG neurons from WT and *TRPV1*$^{-/-}$ mice for different conditions of pretreatment (vehicle, DAMGO, and DAMGO and capsaicin at 37°C) as also described in Fig. 4A. Inset: TRPV1 current elicited by 100 nM capsaicin at a holding potential of −80 mV. Data are representative of three independent experiments. (**D**) Percentage of peak current inhibition recorded in the experiment represented in (C), treated as indicated. Data are means ± SEM from three independent experiments, from (left to right) 8, 7, 8, 8, 6, and 15 DRG neurons. *$P < 0.01$ by one-way ANOVA and Bonferroni post hoc test.

and competitive opioid receptor antagonist, delayed the recovery time as attested by the increased PWT from day 6 to day 10 in both male (Fig. 6, A and B) and female mice (fig. S5, A and B). In *TRPV1*$^{-/-}$ mice, we found that PWT was decreased by 40% at day 4 and then recovered gradually until day 14. Treatment with Nal-M in both *TRPV1*$^{-/-}$ male (Fig. 6, A and B) and female mice (fig. S5, A and B) had no effect on PWT at any time of the treatment. This absence of endogenous opioid analgesia in *TRPV1*$^{-/-}$ mice was due neither to a difference in inflammation (edema was similar between WT and knockout mice) nor to the capacity of pain-modulating immune cells to produce endogenous opioids and infiltrate the inflamed paw at day 8 of CFA (fig. S6, A to C). Thus, as previously reported, local opioid receptor signaling is fine-tuned by inflammation (*34*), and our results indicate that TRPV1 is a central contributor to this process.

TRPV1 prevents peripheral desensitization of opioid-induced analgesia

To determine whether TRPV1 contributes to the increased efficacy of exogenous opioids in inflammatory conditions (*36*), we used an in vivo paradigm of acute opioid receptor desensitization induced by repetitive injection of morphine (10 mg/kg intraperitoneally, twice daily for 3 days; Fig. 7A). We then assessed the dose response of morphine analgesia in CFA-inflamed mice, treated or not with morphine for 3 days. To distinguish central versus peripheral effects, we determined morphine potency [median effective dose (ED_{50})] in mice that were given escalating doses of morphine via intrathecal (central) or local (peripheral) injection into the inflamed paw (Fig. 7, B and C). When administered intrathecally in morphine-naïve mice, morphine dose-dependently attenuated CFA-induced mechanical hypersensitivity: The ED_{50} was comparable in WT and *TRPV1*$^{-/-}$ mice, suggesting that TRPV1 did not alter morphine antinociceptive potency in mice without previous exposure to morphine (Fig. 7C). In other words, acute morphine antinociception was not affected by the absence of TRPV1. By contrast, after repeated morphine treatment, there was a notable reduction in morphine antinociceptive potency (meaning, increased ED_{50}) (Fig. 7B), suggesting a decreased capacity of MOR to respond to morphine. When administered locally in the inflamed paw of saline-treated CFA-inflamed mice, morphine dose-dependently reduced mechanical hypersensitivity (Fig. 7D), thus confirming previous work that peripheral opioid receptors mitigate inflammatory pain under basal conditions (*6*, *37*, *38*). However, as opposed to what is observed centrally, peripheral morphine potency was maintained in chronic morphine-treated WT mice (Fig. 7, D and E). This result indicated that local inflammation prevents peripheral MOR desensitization upon chronic morphine treatment. This effect is dependent on the presence of TRPV1, as *TRPV1*$^{-/-}$ mice exhibit a decrease in peripheral morphine potency (increased ED_{50}) as observed for centrally administered morphine (Fig. 7, D and E). Thus, our findings show that TRPV1 is responsible for maintaining peripheral opioid receptor signaling in nociceptors in the setting of inflammation. Overall, our results suggest a model wherein activation of TRPV1 during an inflammatory insult translocates β-arrestin2 to the nucleus, which in turn prevents opioid-induced recruitment of β-arrestin2 to MOR and ensues receptor desensitization, thus increasing opioid potency at peripheral nociceptors.

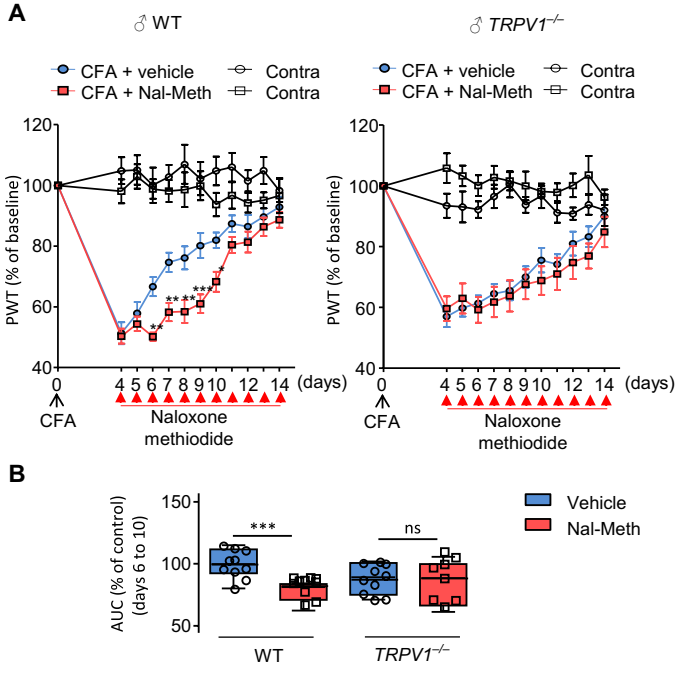

Fig. 6. Peripheral endogenous opioidergic control of inflammatory pain is absent in TRPV1-deficient mice. (**A**) Mechanical sensitivity in mice assessed by PWTs using a dynamic plantar aesthesiometer. CFA was injected into the plantar surface of the right hind paw of WT (left graph) or *TRPV1*$^{-/-}$ (right) male mice. Mice received daily injections of 10 μl of either PBS (blue circles; 10 mice per group) or Nal-M (Nal-Meth; 2 mg/ml; red squares) (10 WT and 8 *TRPV1*$^{-/-}$ mice per group) in the ipsilateral ankle from days 4 to 14, 30 min before assessment of mechanical threshold. Data are means ± SEM of PWT measured in the inflamed (CFA) ipsilateral paw (color) and saline-injected contralateral paw (gray) normalized to baseline. $^{*}P < 0.05$, $^{**}P < 0.01$, and $^{***}P < 0.001$ by two-way ANOVA and Bonferroni post hoc test. (**B**) Area under the PWT curves in (A) between days 6 and 10 were calculated and presented as the percentage of PWT normalized to vehicle-treated animals for each genotype. Data are means, min-max. $^{***}P < 0.001$ (or not significant) by Mann-Whitney *U* test.

DISCUSSION

Previous studies proposed a positive modulation of opioid analgesia in inflammation (*9*, *39*), whereas maladaptive processes occurring during resolution, combined with genetic and emotional predisposition, precipitate the transition to opioid-insensitive chronic pain. Our findings shed light on the functional interplay between inflammation and opioid analgesia, together with the mechanisms that lead to acute and/or persistent receptor desensitization.

The main finding of our work is that activation of the TRPV1 acutely results in the trafficking of β-arrestin2 from the cytosol to the nucleus. This channel-induced translocation attenuates the ability of β-arrestin2 to mediate MOR desensitization, thereby maintaining the sensitivity of MOR-expressing nociceptors to the action of endogenously produced or exogenously administered opioids (Fig. 8). Furthermore, this mechanism of receptor regulation might be shared among other nociceptor-expressed GPCRs, such as PAR2, that are localized in TRPV1-enriched membrane microdomains.

Of relevance to our observations, a number of studies have highlighted TRPV1 as a key effector of MOR, which is supported by the fact that both are expressed in small, unmyelinated DRG neurons (*40*). A substantial proportion of morphine analgesia is mediated by

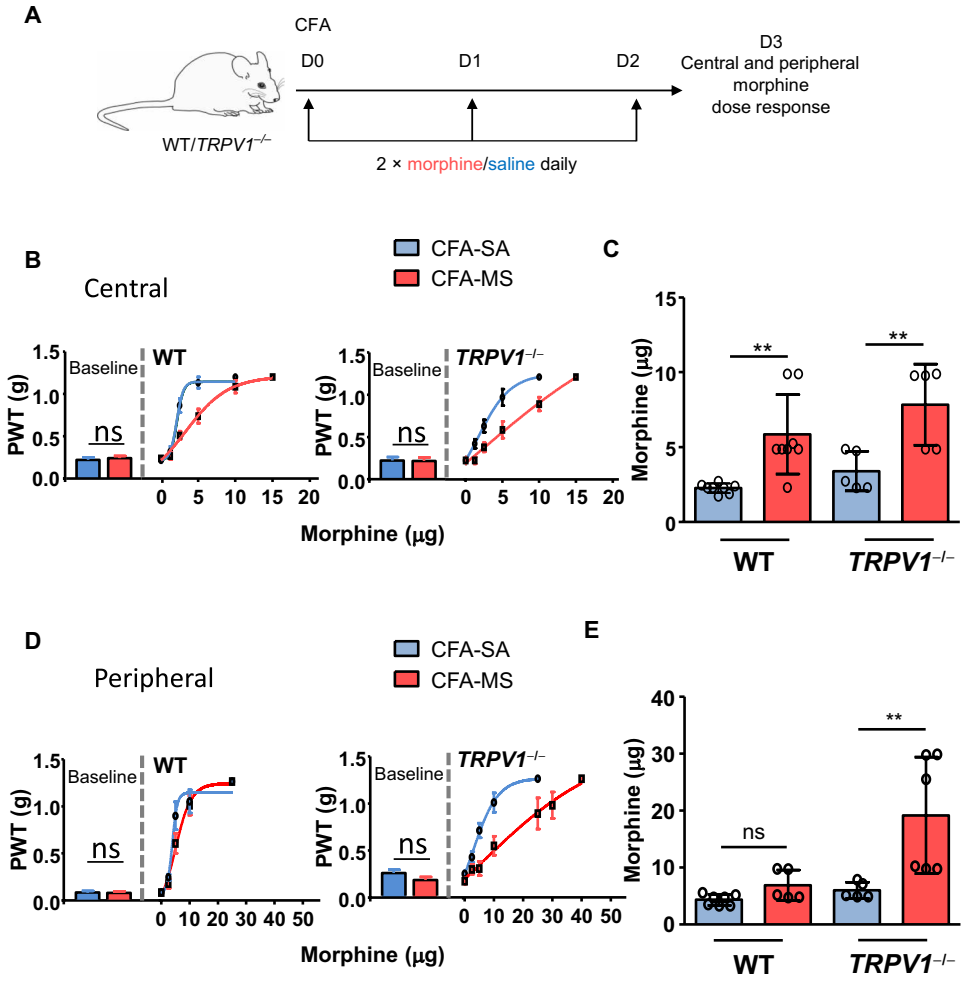

Fig. 7. TRPV1 prevents peripheral opioid desensitization. (**A**) Schematic illustration of the drug administration paradigm. Mice (WT or *TRPV1*$^{-/-}$) were treated with CFA at day 0 (D0) and received two daily injections of a morphine or saline solution (10 mg/kg). On day 3, potency of peripheral opioid–mediated analgesia was evaluated by measuring antinociceptive action of escalating doses of central (intrathecal) or local (paw) injection of morphine. (**B**) Dose-response curve of intrathecal morphine in WT (left) and *TRPV1*$^{-/-}$ (right) mice treated for 3 days after CFA injection with saline (CFA-SA; blue line) or morphine solution (MS; red line). (**C**) ED_{50} values as measured on day 3 after CFA treatment, from (B) (WT mice, $n = 8$; *TRPV1*$^{-/-}$ mice, $n = 5$). (**D** and **E**) As in (B) and (C), except for peripheral (paw) injection of morphine solution. (E: WT-CFA-Saline, $n = 7$; WT-CFA-MS, $n = 5$/TRPV1-CFA-Saline, $n = 5$; TRPV1-CFA-MS, $n = 6$). Data in (B) to (E) are means ± SD; each symbol represents one mouse. $^{**}P < 0.01$ by regular two-way ANOVA and Sidak's post hoc test.

MORs on primary sensory neurons and their central terminals in the spinal cord where TRPV1 is also found. Thus, on one hand, acute morphine administration decreases the capsaicin-induced TRPV1 current (*41*) and reduces the insertion of functional TRPV1 channels into the plasma membrane (*42*), whereas on the other hand, sustained morphine treatment may cause tolerance through the regulation of TRPV1 abundance (*43*). Here, our work reveals a reciprocal regulation of MOR by TRPV1 and identifies the molecular underpinnings of this process involving the TRPV1-triggered translocation of β-arrestin2 to the nucleus. We found that *TRPV1*$^{-/-}$ mice were insensitive to endogenous opioid analgesia during the resolution of inflammation. We then showed that TRPV1 signaling overrode desensitization and maintained peripheral opioid receptor function when using an in vitro or in vivo opioid receptor desensitization paradigm.

TRPV1 agonists, including a capsaicin-containing cream, are extensively used as local analgesics. Although Ca^{2+}-dependent TRPV1 desensitization, inhibition of ion channels, and nerve degeneration have been suggested to contribute to the analgesic effects of capsaicin, these mechanisms remain poorly defined, are reversible, and thus do not explain the long-lasting, pain-relieving effects of capsaicin that persist for weeks after treatment (*44*–*46*). Previous work from Chen and Pan (*47*) determined that RTX-induced ablation of TRPV1-expressing afferent neurons prolonged opioid analgesia despite being accompanied by a reduction in MOR abundance. Nevertheless, our findings suggest that even while maintaining neuronal integrity, TRPV1 activity regulates β-arrestin2 mobilization to fine-tune opioid receptor function when it is most needed. Additional work has described the direct inhibition of VGCCs by capsaicin in DRG neurons (*48*–*50*), which could contribute to decreasing excitatory neurotransmission in the afferent pain pathway. We did not observe such an effect in our hands when preincubating HEK cells or DRG neurons with both DAMGO and capsaicin before washout and recording N-type current inhibition. Furthermore, our BRET analysis suggests

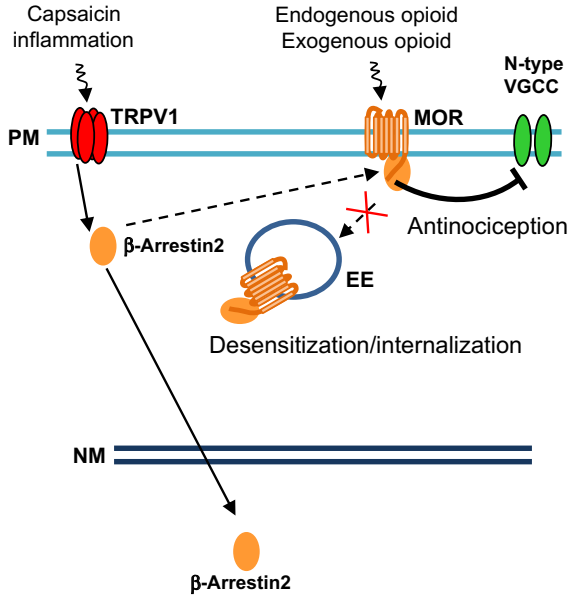

Fig. 8. Model of the TRPV1-MOR interplay during opioid desensitization. Activation of MOR by exogenous or endogenous opioids mediates antinociception through the inhibition of N-type VGCCs in DRG neurons. Receptor desensitization and internalization is mediated by cellular signaling cascades, including the GRK-mediated phosphorylation of MOR, which in turn elicits β-arrestin2–dependent internalization of the receptor into early endosomes. Our data suggest that stimulation of TRPV1 with capsaicin or inflammatory mediators (protons, lipids, and temperature) promotes the translocation of β-arrestin2 to the nucleus and thus prevents MOR desensitization and internalization, facilitating inhibition of N-type channels.

a shift in MOR signaling that was likely caused by the absence of an interaction with β-arrestin2 upon channel activation. Our electrophysiology data indeed indicate that Gβγ (the βγ heterodimer of G proteins)–mediated modulation of N-type current was restored by TRPV1 activation; however, a direct assessment of $G_{i/o}$ coupling to MOR will ascertain whether G protein–biased signaling is favored upon TRPV1 stimulation.

The main target of opioids used in the treatment of acute and chronic pain is represented by MOR, and their effect is mediated partly by inhibition of high voltage–gated N-type channels (*51*). Sustained agonist activation of MOR, however, produces cellular opioid tolerance, which is caused by the β-arrestin2–dependent internalization of MORs that are trafficked to endosomal compartments (*52*). It is well established that receptor desensitization and internalization are two processes that participate, among other mechanisms (including resensitization, down-regulation, or de novo receptor synthesis), in opioid tolerance (*53*–*55*). Therefore, further work will test this TRPV1-MOR paradigm in mouse models of opioid tolerance.

Last, our findings that β-arrestin2 translocates to the nucleus after channel activation will stimulate some new lines of research on the genetic and epigenetic mechanisms of pain modulation by this TRPV1–β-arrestin2 pathway. In contrast to previous studies showing a physical association between β-arrestin2 and TRPV1 (*23*), we could not find evidence of a direct interaction between the two proteins using a BRET assay, and observation by confocal microscopy denoted distinct subcellular localization of the two proteins. β-Arrestin2 was already reported to shuttle from the nucleus to the cytoplasmic compartment (*56*); however, the presence of a nuclear export signal in the 390 to 400 residues of the C-terminal domain excludes β-arrestin2 from the nucleus. Mutations of this motif or pharmacological inhibition of nuclear export promote the translocation of β-arrestin2 into the nucleus (*56*, *57*). Several potential roles of β-arrestin in the nucleus have been proposed, including transcriptional regulation, DNA repair, and histone acetylation (*58*, *59*). The rapid and reversible trafficking of β-arrestin2 to the nucleus is not consistent with apoptotic pathways being engaged by the channel. However, we believe that transcriptional regulation mediated by TRPV1–β-arrestin2 signaling could contribute to the analgesic effect of topical capsaicin formulations used for pain management. Future proteomic and transcriptional studies may advance our knowledge of the factors interacting with β-arrestin2, as well as the genes regulated by TRPV1 signaling. It is likely that β-arrestin2 has an important function in the plasticity of nociceptive circuits after inflammation.

Our data support the findings that TRPV1 activation blocks the opioid-dependent phosphorylation of the MOR by GPCR kinase 5 (GRK5) (*24*). Thus, not only would TRPV1 activation attenuate the GRK-mediated recruitment of β-arrestin2 to trigger MOR desensitization and internalization but also the TRPV1-mediated translocation of β-arrestin2 from the cytosol would also diminish its effect on MOR and likely on other GPCRs present in nociceptors. Together, our work, along with the data of Scherer *et al.* (*24*), support the concept that TRPV1 can bias MOR signaling through a dual mechanism involving the inhibition of receptor phosphorylation and the shuttling of β-arrestin2 to the nucleus.

Although preventing Ca^{2+} influx through TRPV1 blocked β-arrestin2 translocation, increasing the concentration of intracellular Ca^{2+} by activating the Ca^{2+}-permeant channel TRPA1 did not stimulate the nuclear trafficking of β-arrestin2. Therefore, the dynamics of these events will have to be investigated further to understand the spatial and temporal requirements for Ca^{2+} signaling to trigger β-arrestin2 translocation and to determine whether there is cotrafficking of other signaling constituents (for example, GRK5) with β-arrestin2. Inflammation affects the blood-nerve or blood-brain barrier and thereby influences the analgesic action of immune-derived opioids (*60*, *61*). With that in mind, we compared the inflammatory response in *TRPV1*$^{-/-}$ and WT mice. The absence of difference in paw edema, T lymphocyte infiltration, and opioid production (fig. S6) suggested similar inflammatory processes between WT and *TRPV1*$^{-/-}$ mice in response to CFA injection and thus implied that nerve access is unlikely altered in *TRPV1*$^{-/-}$ mice.

Our results suggest a paradigm shift in our understanding of the regulation of opioid receptor function in response to inflammation and the maladaptive processes that could lead to pathological pain during tissue healing. Whereas clinical observations suggest that opioids are effective analgesics after acute injury, prolonged treatment for chronic pain conditions is often accompanied by side effects that may relate to MOR desensitization and the subsequent requirement of higher opioid doses to achieve the same analgesic effect. Our data suggest that dysregulation of the TRPV1–β-arrestin2 signaling pathway could contribute to the transition from acute to chronic pain and highlight TRPV1 channels as potential modulators of opioid analgesia. If used in conjunction with opioids, then TRPV1 agonists might improve the management of chronic and severe morphine-resistant pain by highjacking endogenous mechanisms of receptor desensitization (*62*), potentiating opioid analgesia and thus limiting dose escalation.

MATERIAL AND METHODS

Chemicals and drugs

The TRPV1 agonists RTX and capsaicin were obtained from Sigma-Aldrich. The MAPK inhibitor (U-0126) is from Cell Signaling Technology. The PKC inhibitor CGP53353 and GF109203X were purchased from Tocris Bioscience. Ionomycin was obtained from Alomone Labs.

Mice

Two-month-old C57bl/6 mice were obtained from Jackson Laboratories (Bar Harbor, ME). All mice were housed with a 12-hour light/12-hour dark cycle and under standard conditions with drinking water and food available ad libitum. All experiments were conducted on age-matched animals, under protocols approved by the University of Calgary Animal Care Committee and in accordance with the international guidelines for the ethical use of animals in research and guidelines of the Canadian Council on Animal Care. *TRPV1*$^{-/-}$ mice (strain B6.129X1-Trpv1tm1Jul/J) were originally obtained from the Jackson Laboratories and bred at the University of Calgary Animal Resource Center. Mice were genotyped with the following primers: WT, cctgctcaacatgctcattg [984 base pairs (bp)]; heterozygotes, tcctcatgcacttcaggaaa (450 and 984 bp); and *TRPV1*$^{-/-}$, tggatgtggaat-gtgtgcgag (450 bp; Jackson Laboratories). Transgenic Ai32/TRPV1-cre mice were bred in the University of Calgary Animal Resource Center (G. W. Zamponi) by crossing mice homozygous for the Rosa-CAG-LSL-ChR2 (H134R)-EYFP-WPRE conditional allele (loxP-flanked STOP cassette) [strain B6;129S-Gt(ROSA)26Sortm32(CAG – COP4*H134R/EYFP)Hze/J; hereafter Ai32] with mice expressing Cre recombinase in TRPV1 cells [strain B6.129-Trpv1tm1(cre)Bbm/J; hereafter TRPV1-cre] (both from the Jackson Laboratories).

CFA-induced inflammatory pain

Mice received 20 µl of CFA (1 mg/ml; Sigma, St. Louis, MO) in the right hind paw, as previously described (*61*). They were acclimated to the dynamic plantar aesthesiometer testing chamber for 1 hour, two consecutive days before behavioral testing. From days 4 to 14 after CFA injection, mice received either 10 µl of PBS or Nal-M (2 mg/ml) in the ipsilateral ankle. Mechanical threshold was assessed 30 min after injection. Paw edema was measured throughout the experiment with a plethysmometer (Hugo Basile).

In vivo opioid receptor desensitization paradigm

Mice were injected with CFA or 20 µl of saline as control in the morning. Morphine (10 mg/kg; Professional Compounding Centers of America Corp., London, Ontario, Canada) or 0.9% saline (Sigma) was injected intraperitoneally 1 hour after CFA and then again in the afternoon. Morphine injections were repeated twice daily, for two more consecutive days (day 1 and day 2). On day 3, mechanical nociceptive threshold was determined by the simplified up-and-down method using von Frey filament (*63*) in response to increasing doses of Morphine injected either intrathecally (at doses of 0, 1, 2.5, 5, 10, and 15 µg) or locally (in the ankle, at doses of 0, 2.5, 5, 10, 25, 30, and 40 µg) in the inflamed paw.

Plasmids

TRPV1-YFP and TRPV1-Rluc have been previously described (*14*), TRPA1-YFP was constructed by cloning the TRPA1 coding sequence (a gift from A. Patapoutian) into pEYFP-N1. TRPV1-mCherry and TRPA1-mCherry were produced by cloning the mCherry sequence in place of YFP in TRPV1-pEYFP and TRPA1-pEYFP using (Not I and Kpn I). TRPV1-CFP was generated by replacing the YFP coding sequence of TRPV1-YFP with CFP from pECFP (Clontech). β-Arrestin2–YFP and β2ARR-rLucII have been previously described (*64*). Rat MOR1-YFP, $Ca_v2.2$, Cavβ2a, and α2-δ1 subunits were gifts from G. W. Zamponi. The MOR-YFP plasmid was used to generate MOR1-HA by cloning sticky-ended oligos containing the HA tag (YPYDVPDYA) in place of YFP. MOR-Rluc8 was produced by using polymerase chain reaction (PCR) to introduce Age I and Not I sites to RLuc8 (a gift from M. Bruchas) to clone in place of YFP. β-Arrestin2–Venus was generated as previously described (*65*). PKC-βII–GFP was provided by S. S. G. Ferguson. β-Arrestin2 lentiCRISPR-V2 plasmids were a gift from M. Hollenberg and contained guide sequences identified in a genome-wide screening (*65*). Humanized *Renilla* GFP (*25*) was synthesized (GenScript) and cloned into pcDNA3.1. We added the SV40 large T antigen NLS PKKKRKVEDPKS (*66*) by PCR, using an oligonucleotide containing the C-terminal 24 bp of rGFP (*25*), a 9-bp linker (GGTGGATCC), and the coding sequence of the NLS: CCGAAGAAAAAAAG-GAAGGTTGAAGATCCGAAATCG. Nuclear localization of the resulting construct was confirmed by colocalization with DAPI. The FYVE domain of endofin that localizes to $Rab5^+$ early endosomes was fused to the C terminus of rGFP (rGFP-FYVE) (*25*). Constructs were confirmed with DNA sequencing.

Cell culture and transfection

TsA-201 HEK cells were maintained in Dulbecco's modified Eagle's medium supplemented with 10% FBS (fetal bovine serum), L-glutamine, and penicillin/streptomycin at 37°C in 5% CO_2. Plasmids were transfected using calcium phosphate as previously described (*67*) or Lipofectamine 2000 for the BRET assay (*14*). The pERK assay was done using 1 µg of rat TRPV1 plasmid transfected in a 35-mm dish. Experiments were performed 24 to 48 hours after transfection. For electrophysiology experiments using the β-arrestin2 CRISPR cell line, gene deletion was achieved by using published CRISPR guide RNAs (GAAGTCGAGCCCTAACTGCA and GCGGGACTTCG-TAGATCACC) (*68*) cloned into the lentiCRISPR V2 vector (Addgene plasmid no. 52961). HEK cells were transfected with CRISPR vectors using Lipofectamine LTX (Invitrogen), and cells were selected with puromycin (2.5 µg/ml). Successful β-arrestin2 knockdown was confirmed by Western blotting analysis.

Western blotting analysis

Two days after transfection, cells were stimulated with RTX, harvested, pelleted, and lysed in radioimmunoprecipitation assay (RIPA) lysis buffer (1% Igepal, 0.1% SDS, and 0.5% sodium deoxycholate in PBS) supplemented with a protease and phosphatase inhibitor cocktail (Complete Mini EDTA-free and PhosStop, respectively, Roche). Cleared lysates were separated by SDS–polyacrylamide gel electrophoresis and transferred to nitrocellulose membranes. Membranes were blocked in 5% bovine serum albumin (Sigma) or milk in TBS-T [50 mM tris, 150 mM NaCl, and 0.05% Tween 20 (pH 7.5)] and probed with the following antibodies: ERK, pERK, and β-arrestin2 (C16D9) (all at 1:2000; Cell Signaling) and glyceraldehyde-3-phosphate dehydrogenase (1:1000; Santa Cruz Biotechnology). Horseradish peroxidase–conjugated enhanced chemiluminesence–optimized secondary antibodies (GE Healthcare) were visualized on a Bio-Rad ChemiDoc. For pERK assays, cells were serum-starved for 3 hours before stimulation.

Quantitative PCR assays

Ipsilateral popliteal lymph nodes were harvested at day 3 and day 8 after CFA injection, dissociated using a bullet blender (Next Advance) with SSB05 beads (Next Advance) in RLT buffer (Qiagen, Toronto, Ontario, Canada). Total RNA was extracted using an RNeasy Mini kit (Qiagen), according to the manufacturer's instructions. The quality and quantity of RNA were determined using a NanoDrop 2000c spectrophotometer (Thermo Fisher Scientific, Montréal, Quebec, Canada). Relative Proenkephalin (PENK) gene expression [normalized to hypoxanthine-guanine phosphoribosyltransferase (HPRT)] was determined by quantitative PCR using Quantitect SYBR Green PCR Master Mix (Qiagen) and a StepOnePlus real-time PCR detection system (Applied Biosystems, Burlington, Ontario, Canada). The following primers were used: 5′-GTTCTTTGCTGACCTGCTGGAT-3′ and 5′-CCCCGTTGACTGATCATTACAG-3′ for HPRT, 5′-CGACATCAATTTCCTGGCGT-3′ and 5′-AGATCCTTGCAGGTCTCCCA-3′ for PENK.

Fluorescence-activated cell sorting analysis

At day 8 of CFA, paw tissue was minced and digested in Hanks' balanced salt solution (HBSS) containing collagenase I (1 mg/ml; Roche) and dispase (2.4 U/ml; Gibco) for 90 min at 37°C under agitation. After digestion, cells were filtered through a 70-mm mesh and washed in PBS 1% FBS. After blocking with CD16/CD32 (1/100 Fc Block, eBioscience) on ice for 15 min, cells were stained for 20 min with an anti-mouse CD3–fluorescein isothiocyanate (clone 145-2C11, BD Biosciences) and anti-mouse CD11b-PercP Cy5.5 (clone M1/70, eBioscience) and then analyzed on a BD FACSCanto II (BD Biosciences).

Immunostaining and confocal microscopy

Cells were plated on MatTek dishes coated overnight with poly-ornithine (0.002%), transfected with calcium phosphate, and allowed to express for 48 hours before treatment. Cells were then fixed in 4% paraformaldehyde. Confocal images were collected on a Zeiss LSM-510 Meta inverted microscope using either a 40× water immersion or a 63× oil 1.4 numerical aperture oil immersion lens. Venus/YFP was visualized by excitation with an argon laser (514 nm), and emission was detected using a long-pass 530-nm filter. Enhanced GFP was visualized by excitation at 488 nm. Image acquisition was performed with identical gain, contrast, laser excitation, pinhole aperture, and laser scanning speed.

Immunostaining of β-arrestin2 in DRG neurons was done using the monoclonal β-arrestin2 (SC-13140, Santa Cruz Biotechnology). Alexa Fluor 594 antibody was visualized by excitation with a HeNe laser (543 nm), and emission was detected using a 585- to 615-nm band-pass filter.

Isolation of DRG neurons

DRG neurons were excised from 6-week-old mice (WT or *TRPV1*$^{-/-}$) and enzymatically dissociated in HBSS containing collagenase (2 mg/ml) and dispase (4 mg/ml; Invitrogen) for 45 min at 37°C (*20*). DRGs were rinsed twice in HBSS and once in culture medium consisting of Dulbecco's minimum essential medium supplemented with 10% heat-inactivated FBS, streptomycin (100 μg/ml), penicillin (100 U/ml), and nerve growth factor (100 ng/ml; all from Invitrogen). Individual neurons were dispersed by trituration through a fire-polished glass Pasteur pipette in 4 ml of media. Neurons were cultured on glass coverslips previously treated with HBSS + 25% poly-L-ornithine and laminin (both from Sigma), overnight at 37°C with 5% CO_2 in 96% humidity.

Quantification of MOR internalization and β-arrestin2 nuclear localization

HEK cells cotransfected with a DNA mix of TRPV1-mCherry and MOR-YFP (500 ng each) were treated with vehicle or DAMGO (1 μM). To assess the effect of TRPV1 activation, cells were pretreated with capsaicin (100 nM) for 20 min before DAMGO treatment. Cells were imaged on a Zeiss LSM-510 Meta inverted confocal microscope. Images were then analyzed with ImageJ software, using a sequence of events including background subtraction and transformation of MOR-YFP signal to an 8-bit image, adjusting threshold and noise reduction. Vesicles within the cells were then counted using ImageJ macro. The same sequences of events using identical settings were consistently applied to each image.

To quantify the extent of β-arrestin2 translocation to the nucleus, we transfected HEK cells on coverslips with YFP-βarr2 with or without TRPV1 and allowed the plasmids to express for 48 hours. Cells were then washed in HBSS and stimulated with 1 μM capsaicin for 15 min at 37°C. The 15-min–time point coverslips were fixed, medium was replaced, and then the remaining coverslips were fixed at 30, 60, and 120 min from the beginning of stimulation. Coverslips were mounted on slides using Prolong Gold Antifade with DAPI mountant. Wide-field fluorescent images were acquired on a Zeiss LSM-510 Meta confocal microscope, and we quantified the number of cells in the field of view that showed YFP-βarr2 in the nucleus (indicated by DAPI) and the total number of YFP-βarr2–positive cells.

BRET assay

BRET assay was performed between MOR-Rluc8 and βARR2-Venus, MOR-YFP and βARR2-Rluc, or βARR2-RlucII and PAR2-YFP, as previously described (*14*, *64*). Briefly, HEK cells were cotransfected with a DNA mix of 100 ng: 1 μg (donor-acceptor) (+100 ng of TRPV1, TRPA1, or pCDNA3 as control), using Lipofectamine (Invitrogen). At the next day of transfection, cells were plated in a white 96-well plate (BRAND). The agonist-induced BRET signal was calculated as the difference in BRET signal from cells treated with agonist or vehicle. For the dose-response BRET curve, cells were incubated with different concentrations of DAMGO for 15 min at 37°C and then washed and treated with the RLuc substrate coelenterazine h (5 μM) for 5 min before BRET measurement. BRET signal was measured in a Mithras LB940 (Berthold Technologies) and calculated as the ratio of YFP emission (530 nm) to the RLuc emission at (460 nm). BRET signal was expressed as net BRET, which is the difference between the signal from YFP/RLuc and the signal from RLuc alone.

For BRET assay between MOR-YFP and βARR2-Rluc, cells were transfected in 96-well plates using Lipofectamine 2000 (Invitrogen) with a DNA mix containing 100 ng of MOR-YFP plasmid [provided by S. Granier (Institut de Genomique Fonctionelle Montpellier)] and 2 ng of βARR2-Rluc plasmid [provided by M. G. Scott (Institut Cochin, Paris, France)] and 40 ng of TRPV1 plasmid [obtained from K. Talavera (Leuven, Belgium)] or empty vector. Twenty-four hours after transfection, BRET signal was measured using the pharmacological screening platform of the IGF, ARPEGE (www.arpege.cnrs.fr). Cells were washed twice with PBS and treated with coelanterazine-h (5 μM) for 5 min before stimulation with DAMGO (10 μM) or

capsaicin (500 nM) or DAMGO and capsaicin. For bystander BRET, cells were transfected with a DNA mix of β-arr2-rLuc (100 ng), rGFP-NLS (100 ng), and TRPV1 or TRPA1 (100 ng).

Electrophysiology

Whole-cell patch-clamp experiments on HEK cells were performed 16 to 24 hours after transfection with calcium phosphate (*69*). The internal pipette solution contained the following: 110 mM CsCl, 3 mM $MgCl_2$, 10 mM EGTA, 10 mM Hepes, 5 mM MgATP, and 1 mM GTP (pH 7.2 adjusted with CsOH). The bath solution contained the following: 20 mM $BaCl_2$, 1 mM $MgCl_2$, 10 mM Hepes, 40 mM TEA-Cl, 65 mM CsCl, and 10 mM D-glucose (pH 7.4 adjusted with TEA-OH) for HEK cells and 10 mM $BaCl_2$, 10 mM Hepes, 120 mM TEA-Cl, and 10 mM D-glucose (pH 7.4 adjusted with TEA-OH) for DRG. The DRG recording solution also contained 10 μM nifedipine (Sigma, USA) to inhibit L-type calcium currents. The recording solutions used for TRPV1 currents contained the following: 140 mM NaCl, 1.5 mM $CaCl_2$, 2 mM $MgCl_2$, 5 mM KCl, 10 mM Hepes, and 10 mM D-glucose (pH 7.4 adjusted with NaOH) and the same internal solution mentioned above. In cells that showed TRPV1 currents, the external solution was switched to the barium-containing solution mentioned above to record voltage-gated calcium currents. Patch-clamp experiments were performed using an Axopatch 200B amplifier (Axon Instruments), and pClamp 10.5 software was used for data acquisition and analysis (both from Molecular Devices Corp.). Data were digitized at 10 kHz and low-pass–filtered at 1 kHz. Borosilicate glass (Harvard Apparatus Ltd.) pipettes were pulled and polished to a resistance of 2 to 5 megohms with a DMZ-Universal Puller (Zeitz-Instruments GmbH.). When applicable, voltages were corrected for liquid junction potentials. All experiments were conducted at room temperature (22° ± 2°C).

Immunoprecipitation

For immunoprecipitation, 7.5 μg of TRPV1-HA and MOR1-YFP complementary DNA (cDNA) were cotransfected into tsA201 cells in 10-cm plates at about 50% confluency, using the calcium phosphate method. Cells were harvested 48 hours later into 5 ml of PBS and treated in suspension with 10 μM DAMGO for 15 min at 37°C. Cells were then centrifuged, and the pellet was lysed in RIPA with protease inhibitor (Roche Complete Mini without EDTA) for 1 hour on ice. TRPV1 was immunoprecipitated from lysates using monoclonal anti-HA agarose conjugate (Sigma) overnight at 4°C. Agarose beads with bound protein were washed three times in RIPA; bound proteins were eluted in Laemmli buffer for 30 min at 37°C and run on a tris-glycine gel. Separated proteins were transferred to a nitrocellulose membrane and blotted for HA (1:1000; Covance) and GFP (1:5000; Torrey Pines).

Statistical analysis

Data analysis was completed with Clampfit 10.5 software (Axon Instruments) or GraphPad Prism 7 (GraphPad software). Graphs and statistical analyses for electrophysiology experiments were performed with Origin 7.0 analysis software (OriginLab). Results were expressed as means ± SEM, and SD and numbers in parentheses reflect the number of cells (n). Statistical analyses were completed with either paired t tests for all the results obtained before and after treatment with DAMGO in the same cells or unpaired t tests when data were obtained from different cells. Where appropriate, ANOVA followed by Bonferroni or Sidak's post hoc test were performed. The criterion for statistical significance was set at $P < 0.05$ regardless of the method used.

SUPPLEMENTARY MATERIALS

www.sciencesignaling.org/cgi/content/full/12/575/eaav0711/DC1

Fig. S1. The translocation of β-arrestin2 to the nucleus is dependent on TRPV1 activation and accompanied by a transient PKCβII-dependent phosphorylation of ERK1/2.

Fig. S2. Activation of TRPV1 prevents MOR and PAR2 from interacting with β-arrestin2.

Fig. S3. The nuclear translocation of β-arrestin2 after TRPV1 stimulation is associated with impaired MOR internalization.

Fig. S4. DAMGO and capsaicin have no detectable effects on $Ca_V2.2$ inhibition in the absence of MOR and TRPV1.

Fig. S5. Peripheral endogenous control of inflammatory pain is absent in female TRPV1-deficient mice.

Fig. S6. Paw edema, T lymphocyte infiltration, and opioid production are not altered in *TRPV1*$^{-/-}$ mice.

REFERENCES AND NOTES

1. G. Corder, S. Doolen, R. R. Donahue, M. K. Winter, B. L. Jutras, Y. He, X. Hu, J. S. Wieskopf, J. S. Mogil, D. R. Storm, Z. J. Wang, K. E. McCarson, B. K. Taylor, Constitutive μ-opioid receptor activity leads to long-term endogenous analgesia and dependence. *Science* **341**, 1394–1399 (2013).
2. M. H. Ossipov, G. O. Dussor, F. Porreca, Central modulation of pain. *J. Clin. Invest.* **120**, 3779–3787 (2010).
3. H. Leduc-Pessah, N. L. Weilinger, C. Y. Fan, N. E. Burma, R. J. Thompson, T. Trang, Site-specific regulation of P2X7 receptor function in microglia gates morphine analgesic tolerance. *J. Neurosci.* **37**, 10154–10172 (2017).
4. U. Baddack-Werncke, M. Busch-Dienstfertig, S. González-Rodríguez, S. C. Maddila, J. Grobe, M. Lipp, C. Stein, G. Müller, Cytotoxic T cells modulate inflammation and endogenous opioid analgesia in chronic arthritis. *J. Neuroinflammation* **14**, 30 (2017).
5. J. Boué, L. Basso, N. Cenac, C. Blanpied, M. Rolli-Derkinderen, M. Neunlist, N. Vergnolle, G. Dietrich, Endogenous regulation of visceral pain via production of opioids by colitogenic $CD4^+$ T cells in mice. *Gastroenterology* **146**, 166–175 (2014).
6. J. Boué, C. Blanpied, M. Djata-Cabral, L. Pelletier, N. Vergnolle, G. Dietrich, Immune conditions associated with CD4+ T effector-induced opioid release and analgesia. *Pain* **153**, 485–493 (2012).
7. C. Stein, L. J. Lang, Peripheral mechanisms of opioid analgesia. *Curr. Opin. Pharmacol.* **9**, 3–8 (2009).
8. M. Verma-Gandhu, P. Bercik, Y. Motomura, E. F. Verdu, W. I. Khan, P. A. Blennerhassett, L. Wang, R. T. El-Sharkawy, S. M. Collins, $CD4^+$ T-cell modulation of visceral nociception in mice. *Gastroenterology* **130**, 1721–1728 (2006).
9. E. K. Joseph, D. B. Reichling, J. D. Levine, Shared mechanisms for opioid tolerance and a transition to chronic pain. *J. Neurosci.* **30**, 4660–4666 (2010).
10. C. Stein, J. D. Clark, U. Oh, M. R. Vasko, G. L. Wilcox, A. C. Overland, T. W. Vanderah, R. H. Spencer, Peripheral mechanisms of pain and analgesia. *Brain Res. Rev.* **60**, 90–113 (2009).
11. P. R. Picard, M. R. Tramèr, H. J. McQuay, R. A. Moore, Analgesic efficacy of peripheral opioids (all except intra-articular): A qualitative systematic review of randomised controlled trials. *Pain* **72**, 309–318 (1997).
12. E. Bourinet, C. Altier, M. E. Hildebrand, T. Trang, M. W. Salter, G. W. Zamponi, Calcium-permeable ion channels in pain signaling. *Physiol. Rev.* **94**, 81–140 (2014).
13. K. Bölcskei, Z. Helyes, A. Szabó, K. Sándor, K. Elekes, J. Németh, R. Almási, E. Pintér, G. Pethő, J. Szolcsányi, Investigation of the role of TRPV1 receptors in acute and chronic nociceptive processes using gene-deficient mice. *Pain* **117**, 368–376 (2005).
14. R. Flynn, K. Chapman, M. Iftinca, R. Aboushousha, D. Varela, C. Altier, Targeting the transient receptor potential vanilloid type 1 (TRPV1) assembly domain attenuates inflammation-induced hypersensitivity. *J. Biol. Chem.* **289**, 16675–16687 (2014).
15. R. Planells-Cases, P. Valente, A. Ferrer-Montiel, F. Qin, A. Szallasi, Complex regulation of TRPV1 and related thermo-TRPs: Implications for therapeutic intervention. *Adv. Exp. Med. Biol.* **704**, 491–515 (2011).
16. J. Siemens, S. Zhou, R. Piskorowski, T. Nikai, E. A. Lumpkin, A. I. Basbaum, D. King, D. Julius, Spider toxins activate the capsaicin receptor to produce inflammatory pain. *Nature* **444**, 208–212 (2006).
17. M. Tominaga, M. J. Caterina, A. B. Malmberg, T. A. Rosen, H. Gilbert, K. Skinner, B. E. Raumann, A. I. Basbaum, D. Julius, The cloned capsaicin receptor integrates multiple pain-producing stimuli. *Neuron* **21**, 531–543 (1998).
18. L. Basso, T. K. Lapointe, M. Iftinca, C. Marsters, M. D. Hollenberg, D. M. Kurrasch, C. Altier, Granulocyte-colony–stimulating factor (G-CSF) signaling in spinal microglia drives visceral sensitization following colitis. *Proc. Natl. Acad. Sci. U.S.A.* **114**, 11235–11240 (2017).

19. P. Delmas, SnapShot: Ion channels and pain. *Cell* **134**, 366–366.e1 (2008).
20. T. K. Lapointe, L. Basso, M. C. Iftinca, R. Flynn, K. Chapman, G. Dietrich, N. Vergnolle, C. Altier, TRPV1 sensitization mediates postinflammatory visceral pain following acute colitis. *Am. J. Physiol. Gastrointest. Liver Physiol.* **309**, G87–G99 (2015).
21. J. Vriens, G. Appendino, B. Nilius, Pharmacology of vanilloid transient receptor potential cation channels. *Mol. Pharmacol.* **75**, 1262–1279 (2009).
22. G. Corder, V. L. Tawfik, D. Wang, E. I. Sypek, S. A. Low, J. R. Dickinson, C. Sotoudeh, J. D. Clark, B. A. Barres, C. J. Bohlen, G. Scherrer, Loss of μ opioid receptor signaling in nociceptors, but not microglia, abrogates morphine tolerance without disrupting analgesia. *Nat. Med.* **23**, 164–173 (2017).
23. E. D. Por, S. M. Bierbower, K. A. Berg, R. Gomez, A. N. Akopian, W. C. Wetsel, N. A. Jeske, β-arrestin-2 desensitizes the transient receptor potential vanilloid 1 (TRPV1) channel. *J. Biol. Chem.* **287**, 37552–37563 (2012).
24. P. C. Scherer, N. W. Zaccor, N. M. Neumann, C. Vasavda, R. Barrow, A. J. Ewald, F. Rao, C. J. Sumner, S. H. Snyder, TRPV1 is a physiological regulator of μ-opioid receptors. *Proc. Natl. Acad. Sci. U.S.A.* **114**, 13561–13566 (2017).
25. Y. Namkung, C. Le Gouill, V. Lukashova, H. Kobayashi, M. Hogue, E. Khoury, M. Song, M. Bouvier, S. A. Laporte, Monitoring G protein-coupled receptor and β-arrestin trafficking in live cells using enhanced bystander BRET. *Nat. Commun.* **7**, 12178 (2016).
26. Y.-S. Park, N. J. Cho, EGFR and PKC are involved in the activation of ERK1/2 and p90 RSK and the subsequent proliferation of SNU-407 colon cancer cells by muscarinic acetylcholine receptors. *Mol. Cell. Biochem.* **370**, 191–198 (2012).
27. L. Scapoli, M. E. Ramos-Nino, M. Martinelli, B. T. Mossman, Src-dependent ERK5 and Src/EGFR-dependent ERK1/2 activation is required for cell proliferation by asbestos. *Oncogene* **23**, 805–813 (2004).
28. M. J. Caterina, A. Leffler, A. B. Malmberg, W. J. Martin, J. Trafton, K. R. Petersen-Zeitz, M. Koltzenburg, A. I. Basbaum, D. Julius, Impaired nociception and pain sensation in mice lacking the capsaicin receptor. *Science* **288**, 306–313 (2000).
29. M. Cui, P. Honore, C. Zhong, D. Gauvin, J. Mikusa, G. Hernandez, P. Chandran, A. Gomtsyan, B. Brown, E. K. Bayburt, K. Marsh, B. Bianchi, H. McDonald, W. Niforatos, T. R. Neelands, R. B. Moreland, M. W. Decker, C.-H. Lee, J. P. Sullivan, C. R. Faltynek, TRPV1 receptors in the CNS play a key role in broad-spectrum analgesia of TRPV1 antagonists. *J. Neurosci.* **26**, 9385–9393 (2006).
30. J. B. Davis, J. Gray, M. J. Gunthorpe, J. P. Hatcher, P. T. Davey, P. Overend, M. H. Harries, J. Latcham, C. Clapham, K. Atkinson, S. A. Hughes, K. Rance, E. Grau, A. J. Harper, P. L. Pugh, D. C. Rogers, S. Bingham, A. Randall, S. A. Sheardown, Vanilloid receptor-1 is essential for inflammatory thermal hyperalgesia. *Nature* **405**, 183–187 (2000).
31. C. Brenneis, K. Kistner, M. Puopolo, D. Segal, D. Roberson, M. Sisignano, S. Labocha, N. Ferreirós, A. Strominger, E. J. Cobos, N. Ghasemlou, G. Geisslinger, P. W. Reeh, B. P. Bean, C. J. Woolf, Phenotyping the function of TRPV1-expressing sensory neurons by targeted axonal silencing. *J. Neurosci.* **33**, 315–326 (2013).
32. L. Basso, J. Boué, K. Mahiddine, C. Blanpied, S. Robiou-du-Pont, N. Vergnolle, C. Deraison, G. Dietrich, Endogenous analgesia mediated by $CD4^+$ T lymphocytes is dependent on enkephalins in mice. *J. Neuroinflammation* **13**, 132 (2016).
33. J. Boué, C. Blanpied, P. Brousset, N. Vergnolle, G. Dietrich, Endogenous opioid-mediated analgesia is dependent on adaptive T cell response in mice. *J. Immunol.* **186**, 5078–5084 (2011).
34. C. Stein, H. Machelska, Modulation of peripheral sensory neurons by the immune system: Implications for pain therapy. *Pharmacol. Rev.* **63**, 860–881 (2011).
35. Y.-L. Jiang, X.-F. He, Y.-F. Shen, X.-H. Yin, J.-Y. Du, Y. Liang, J.-Q. Fang, Analgesic roles of peripheral intrinsic met-enkephalin and dynorphin A in long-lasting inflammatory pain induced by complete Freund's adjuvant in rats. *Exp. Ther. Med.* **9**, 2344–2348 (2015).
36. C. Zöllner, S. A. Mousa, O. Fischer, H. L. Rittner, M. Shaqura, A. Brack, M. Shakibaei, W. Binder, F. Urban, C. Stein, M. Schäfer, Chronic morphine use does not induce peripheral tolerance in a rat model of inflammatory pain. *J. Clin. Invest.* **118**, 1065–1073 (2008).
37. Q.-S. Auh, Y. H. Chun, O. K. Melemedjian, Y. Zhang, J. Y. Ro, Peripheral interactions between cannabinoid and opioid receptor agonists in a model of inflammatory mechanical hyperalgesia. *Brain Res. Bull.* **125**, 211–217 (2016).
38. Q.-S. Auh, J. Y. Ro, Effects of peripheral κ opioid receptor activation on inflammatory mechanical hyperalgesia in male and female rats. *Neurosci. Lett.* **524**, 111–115 (2012).
39. R. W. Hurley, D. L. Hammond, The analgesic effects of supraspinal μ and δ opioid receptor agonists are potentiated during persistent inflammation. *J. Neurosci.* **20**, 1249–1259 (2000).
40. G. Scherrer, N. Imamachi, Y. Q. Cao, C. Contet, F. Mennicken, D. O'Donnell, B. L. Kieffer, A. I. Basbaum, Dissociation of the opioid receptor mechanisms that control mechanical and heat pain. *Cell* **137**, 1148–1159 (2009).
41. J. Endres-Becker, P. A. Heppenstall, S. A. Mousa, D. Labuz, A. Oksche, M. Schäfer, C. Stein, C. Zöllner, μ-Opioid receptor activation modulates transient receptor potential vanilloid 1 (TRPV1) currents in sensory neurons in a model of inflammatory pain. *Mol. Pharmacol.* **71**, 12–18 (2007).
42. I. Vetter, W. Cheng, M. Peiris, B. D. Wyse, S. J. Roberts-Thomson, J. Zheng, G. R. Monteith, P. J. Cabot, Rapid, opioid-sensitive mechanisms involved in transient receptor potential vanilloid 1 sensitization. *J. Biol. Chem.* **283**, 19540–19550 (2008).
43. Y. Chen, C. Geis, C. Sommer, Activation of TRPV1 contributes to morphine tolerance: Involvement of the mitogen-activated protein kinase signaling pathway. *J. Neurosci.* **28**, 5836–5845 (2008).
44. V. Carnevale, T. Rohacs, TRPV1: A target for rational drug design. *Pharmaceuticals* **9**, 52 (2016).
45. M.-K. Chung, J. N. Campbell, Use of capsaicin to treat pain: Mechanistic and therapeutic considerations. *Pharmaceuticals* **9**, 66 (2016).
46. B. Nilius, A. Szallasi, Transient receptor potential channels as drug targets: From the science of basic research to the art of medicine. *Pharmacol. Rev.* **66**, 676–814 (2014).
47. S.-R. Chen, H.-L. Pan, Loss of TRPV1-expressing sensory neurons reduces spinal μ opioid receptors but paradoxically potentiates opioid analgesia. *J. Neurophysiol.* **95**, 3086–3096 (2006).
48. T. Hagenacker, F. Splettstoesser, W. Greffrath, R.-D. Treede, D. Büsselberg, Capsaicin differentially modulates voltage-activated calcium channel currents in dorsal root ganglion neurones of rats. *Brain Res.* **1062**, 74–85 (2005).
49. Z.-Z. Wu, S.-R. Chen, H.-L. Pan, Transient receptor potential vanilloid type 1 activation down-regulates voltage-gated calcium channels through calcium-dependent calcineurin in sensory neurons. *J. Biol. Chem.* **280**, 18142–18151 (2005).
50. Z.-Z. Wu, S.-R. Chen, H.-L. Pan, Signaling mechanisms of down-regulation of voltage-activated Ca^{2+} channels by transient receptor potential vanilloid type 1 stimulation with olvanil in primary sensory neurons. *Neuroscience* **141**, 407–419 (2006).
51. Z.-Z. Wu, S.-R. Chen, H.-L. Pan, Differential sensitivity of N- and P/Q-type Ca^2+ channel currents to a μ opioid in isolectin B -positive and -negative dorsal root ganglion neurons. *J. Pharmacol. Exp. Ther.* **311**, 939–947 (2004).
52. S. Allouche, F. Noble, N. Marie, Opioid receptor desensitization: Mechanisms and its link to tolerance. *Front. Pharmacol.* **5**, 280 (2014).
53. L. M. Bohn, R. J. Lefkowitz, R. R. Gainetdinov, K. Peppel, M. G. Caron, F.-T. Lin, Enhanced morphine analgesia in mice lacking β-arrestin 2. *Science* **286**, 2495–2498 (1999).
54. C. M. Cahill, W. Walwyn, A. M. W. Taylor, A. A. A. Pradhan, C. J. Evans, Allostatic mechanisms of opioid tolerance beyond desensitization and downregulation. *Trends Pharmacol. Sci.* **37**, 963–976 (2016).
55. J. T. Williams, S. L. Ingram, G. Henderson, C. Chavkin, M. von Zastrow, S. Schulz, T. Koch, C. J. Evans, M. J. Christie, Regulation of μ-opioid receptors: Desensitization, phosphorylation, internalization, and tolerance. *Pharmacol. Rev.* **65**, 223–254 (2013).
56. P. Wang, Y. Wu, X. Ge, L. Ma, G. Pei, Subcellular localization of β-arrestins is determined by their intact N domain and the nuclear export signal at the C terminus. *J. Biol. Chem.* **278**, 11648–11653 (2003).
57. M. G. H. Scott, E. Le Rouzic, A. Périanin, V. Pierotti, H. Enslen, S. Benichou, S. Marullo, A. Benmerah, Differential nucleocytoplasmic shuttling of β-arrestins. Characterization of a leucine-rich nuclear export signal in β-arrestin2. *J. Biol. Chem.* **277**, 37693–37701 (2002).
58. J. Kang, Y. Shi, B. Xiang, B. Qu, W. Su, M. Zhu, M. Zhang, G. Bao, F. Wang, X. Zhang, R. Yang, F. Fan, X. Chen, G. Pei, L. Ma, A nuclear function of β-arrestin1 in GPCR signaling: Regulation of histone acetylation and gene transcription. *Cell* **123**, 833–847 (2005).
59. E. M. Neuhaus, A. Mashukova, J. Barbour, D. Wolters, H. Hatt, Novel function of β-arrestin2 in the nucleus of mature spermatozoa. *J. Cell Sci.* **119**, 3047–3056 (2006).
60. I. Antonijevic, S. A. Mousa, M. Schafer, C. Stein, Perineurial defect and peripheral opioid analgesia in inflammation. *J. Neurosci.* **15**, 165–172 (1995).
61. H. L. Rittner, S. Amasheh, R. Moshourab, D. Hackel, R.-S. Yamdeu, S. A. Mousa, M. Fromm, C. Stein, A. Brack, Modulation of tight junction proteins in the perineurium to facilitate peripheral opioid analgesia. *Anesthesiology* **116**, 1323–1334 (2012).
62. D. Clauw, Hijacking the endogenous opioid system to treat pain: Who thought it would be so complicated? *Pain* **158**, 2283–2284 (2017).
63. R. P. Bonin, C. Bories, Y. De Koninck, A simplified up-down method (SUDO) for measuring mechanical nociception in rodents using von Frey filaments. *Mol. Pain* **10**, 26 (2014).
64. R. Ramachandran, K. Mihara, H. Chung, B. Renaux, C. S. Lau, D. A. Muruve, K. A. DeFea, M. Bouvier, M. D. Hollenberg, Neutrophil elastase acts as a biased agonist for proteinase-activated receptor-2 (PAR2). *J. Biol. Chem.* **286**, 24638–24648 (2011).
65. S. A. Vishnivetskiy, L. E. Gimenez, D. J. Francis, S. M. Hanson, W. L. Hubbell, C. S. Klug, V. V. Gurevich, Few residues within an extensive binding interface drive receptor interaction and determine the specificity of arrestin proteins. *J. Biol. Chem.* **286**, 24288–24299 (2011).
66. C. L. Wolfe, A. K. Hopper, N. C. Martin, Mechanisms leading to and the consequences of altering the normal distribution of ATP(CTP):tRNA nucleotidyltransferase in yeast. *J. Biol. Chem.* **271**, 4679–4686 (1996).
67. M. Iftinca, R. Flynn, L. Basso, H. Melo, R. Aboushousha, L. Taylor, C. Altier, The stress protein heat shock cognate 70 (Hsc70) inhibits the transient receptor potential vanilloid type 1 (TRPV1) channel. *Mol. Pain* **12**, 1744806916663945 (2016).
68. O. Shalem, N. E. Sanjana, E. Hartenian, X. Shi, D. A. Scott, T. S. Mikkelsen, D. Heckl, B. L. Ebert, D. E. Root, J. G. Doench, F. Zhang, Genome-scale CRISPR-Cas9 knockout screening in human cells. *Science* **343**, 84–87 (2014).

69. T. Hermosilla, C. Moreno, M. Itfinca, C. Altier, R. Armisén, A. Stutzin, G. W. Zamponi, D. Varela, L-type calcium channel β subunit modulates angiotensin II responses in cardiomyocytes. *Channels* **5**, 280–286 (2011).

Acknowledgments: We thank G. Pineyro for technical assistance with the BRET assay, M. Bruchas for the β-arrestin2–Venus and pRLuc8 plasmids, and S. Laporte for the gift of the FYVE-rLuc and rGFP plasmids. We thank G. Zamponi for providing the Ai32/TRPV1-cre mice and the MOR1-YFP cDNA. We thank K. K. H. Poon and the Nicole Perkins Microbial Communities Core Labs for technical assistance with fluorescence-activated cell sorting acquisition. **Funding:** This work was supported by operating grants from the Canadian Institutes of Health Research (CIHR) (to C.A., M.D.H., R.T., and T.T.) by the Vi Riddell Child Pain program of the Alberta Children's Hospital Research Institute (to C.A. and T.T.), by the Fondation pour la Recherche Médicale (équipe FRM 2015) (to E.B.), and by the Agence Nationale pour la Recherche (ANR15-CE16-0012-01) (to E.B.). C.A. holds a Canada Research Chair in inflammatory Pain (Tier2). L.B. holds an ACHRI fellowship from the University of Calgary and a Cumming School of Medicine fellowship from the University of Calgary. **Author contributions:** C.A. conceived the study. L.B., R.A., M.I., R.F., E.B., T.T., and C.A. designed the experiments. L.B., R.A., H.M., C.Y.F., F.A., R.F., and M.I. performed the experiments. L.B., R.A., C.Y.F., F.A., M.I., R.F., and C.A. analyzed the data. L.B., R.A., M.I., R.F., and C.A. wrote the paper with editorial input from M.D.H., E.B., R.T., and T.T. **Competing interests:** The authors declare that they have no competing interests. **Data and materials availability:** All data needed to evaluate the conclusions in the paper are present in the paper or the Supplementary Materials.

Submitted 13 August 2018
Accepted 7 March 2019
Published 2 April 2019
10.1126/scisignal.aav0711

Citation: L. Basso, R. Aboushousha, C. Y. Fan, M. Iftinca, H. Melo, R. Flynn, F. Agosti, M. D. Hollenberg, R. Thompson, E. Bourinet, T. Trang, C. Altier, TRPV1 promotes opioid analgesia during inflammation. *Sci. Signal.* **12**, eaav0711 (2019).

TRPV1 promotes opioid analgesia during inflammation

Lilian Basso, Reem Aboushousha, Churmy Yong Fan, Mircea Iftinca, Helvira Melo, Robyn Flynn, Francina Agosti, Morley D. Hollenberg, Roger Thompson, Emmanuel Bourinet, Tuan Trang and Christophe Altier

Sci. Signal. **12** (575), eaav0711.
DOI: 10.1126/scisignal.aav0711

Analgesic TRPV1

Opiates provide pain relief, but they are addictive, and patients often become desensitized to them and then require greater doses. Inflammation, which is common with painful injuries, enhances the analgesic efficacy of opioids. Basso *et al*. found that inflammation-induced activation of the channel TRPV1 promoted opioid sensitivity and analgesia in mice by relocalizing the protein β-arrestin2 within the cell such that it could not interact with the μ-opioid receptor and facilitate its desensitization. This finding potentially explains the analgesic effect of inflammation in patients taking opioids and may identify ways to therapeutically prevent the need for opiate dose escalation.